Received: 16 November 2023 | Revised: 26 April 2024 | Accepted: 28 April 2024

DOI: 10.1002/dad2.12601

Alzheimer's & Dementia
Diagnosis, Assessment & Disease Monitoring

RESEARCH ARTICLE

Early-phase amyloid PET reproduces metabolic signatures of cognitive decline in Parkinson's disease

William W. T. Aye[1,2] | **Megan R. Stark**[1] | **Kyla-Louise Horne**[1,2] | **Leslie Livingston**[1] | **Sophie Grenfell**[1] | **Daniel J. Myall**[1] | **Toni L. Pitcher**[1,2] | **Mustafa M. Almuqbel**[1,3] | **Ross J. Keenan**[1,3] | **Wassilios G. Meissner**[1,4,5] | **John C. Dalrymple-Alford**[1,6] | **Tim J. Anderson**[1,2,7] | **Campbell Le Heron**[1,2,6,7] | **Tracy R. Melzer**[1,2,3,6]

[1]New Zealand Brain Research Institute, Christchurch, New Zealand

[2]Department of Medicine, University of Otago, Christchurch, New Zealand

[3]Radiology Holding Company New Zealand, Christchurch, New Zealand

[4]CHU Bordeaux, Service de Neurologie des Maladies Neurodégénératives, IMNc, NS-Park/FCRIN Network, Bordeaux, France

[5]Univ. Bordeaux, CNRS, IMN, Bordeaux, France

[6]School of Psychology, Speech and Hearing, University of Canterbury, Psychology, Speech and Hearing Arts Road, Ilam, Christchurch, New Zealand

[7]Department of Neurology, Canterbury District Health Board, Christchurch, New Zealand

Correspondence
William W. T. Aye, New Zealand Brain Research Institute, 66 Stewart Street, Christchurch 8011, New Zealand.
Email: will.aye@nzbri.org

Abstract

INTRODUCTION: Recent work suggests that amyloid beta (Aβ) positron emission tomography (PET) tracer uptake shortly after injection ("early phase") reflects brain metabolism and perfusion. We assessed this modality in a predominantly amyloid-negative neurodegenerative condition, Parkinson's disease (PD), and hypothesized that early-phase ^{18}F-florbetaben (eFBB) uptake would reproduce characteristic hypometabolism and hypoperfusion patterns associated with cognitive decline in PD.

METHODS: One hundred fifteen PD patients across the spectrum of cognitive impairment underwent dual-phase Aβ PET, structural and arterial spin labeling (ASL) magnetic resonance imaging (MRI), and neuropsychological assessments. Multiple linear regression models compared eFBB uptake to cognitive performance and ASL MRI perfusion.

RESULTS: Reduced eFBB uptake was associated with cognitive performance in brain regions previously linked to hypometabolism-associated cognitive decline in PD, independent of amyloid status. Furthermore, eFBB uptake correlated with cerebral perfusion across widespread regions.

DISCUSSION: EFBB uptake is a potential surrogate measure for cerebral perfusion/metabolism. A dual-phase PET imaging approach may serve as a clinical tool for assessing cognitive impairment.

KEYWORDS
arterial spin labeling, cognitive impairment, dementia, early-phase positron emission tomography, magnetic resonance imaging, neurodegenerative disorders, neuroimaging, Parkinson's disease, positron emission tomography

Tracy R. Melzer and Campbell Le Heron contributed equally to this study.

Highlights

- Images taken at amyloid beta (Aβ) positron emission tomography tracer injection may reflect brain perfusion and metabolism.
- Parkinson's disease (PD) is a predominantly amyloid-negative condition.
- Early-phase florbetaben (eFBB) in PD was associated with cognitive performance.
- eFBB uptake reflects hypometabolism-related cognitive decline in PD.
- eFBB correlated with arterial spin labeling magnetic resonance imaging measured cerebral perfusion.
- eFBB distinguished dementia from normal cognition and mild cognitive impairment.
- Findings were independent of late-phase Aβ burden.
- Thus, eFBB may serve as a surrogate measure for brain metabolism/perfusion.

1 | INTRODUCTION

Establishing practical and effective diagnostic pathways for people with cognitive impairment is a crucial international research priority.[1,2] Providing an early and timely diagnosis is critical for patient-centered outcomes, while delays in diagnosing the cause of cognitive impairment can be detrimental.[3,4] Furthermore, implementing emerging therapies aiming to modify the course of Alzheimer's disease (AD) will require early identification of AD pathology, meaning tests for molecular markers of AD will need to feature early in any diagnostic pathway.[2,5,6]

Clinically validated in vivo biomarkers of underlying AD molecular pathology include amyloid beta (Aβ) positron emission tomography (PET) imaging and cerebrospinal fluid (CSF) analysis for amyloid species and phosphorylated tau.[7–11] Aβ PET imaging maintains some clear advantages over CSF analysis, including lower interventional and systems requirements. However, limitations remain with this technique beyond access and expense.[12,13] A negative Aβ PET result effectively excludes AD but provides no further information regarding potential alternative causes of cognitive symptoms, including other neurodegenerative conditions or primarily psychological processes.[14–16] Furthermore, the presence of brain amyloid pathology increases with age and is observed in other neurodegenerative conditions; thus, a clinically positive scan does not always equate to AD as the cause of clinical symptoms.[17–19] Measures of Aβ levels in those who are Aβ positive are also not necessarily predictive of future cognitive trajectories, but measures of brain metabolism (^{18}F fluorodeoxyglucose [^{18}F-FDG] PET) and perfusion (single-photo emission computed tomography and arterial spin labeling [ASL] magnetic resonance imaging [MRI]) may provide more information about differential diagnosis and disease trajectories.[20–26]

Such metabolic or perfusion information is not provided by traditional (i.e., late-phase) Aβ PET scans that assess amyloid accumulation (for ^{18}F-based tracers, generally acquired ≈ 90–110 minutes after radiotracer injection). However, recent work indicates that radiotracer uptake in the minutes after injection (i.e., early phase) might provide a surrogate measure of underlying brain metabolism and blood flow—closely linked measures in the context of neurodegeneration by flow-metabolism coupling.[27–29] Studies have reported positive correlations ($r > 0.7$) between early-phase Aβ PET (including Pittsburgh compound B [PiB] and multiple ^{18}F ligands) and FDG PET across the AD spectrum, from healthy, Aβ-negative controls to Aβ-positive individuals with dementia, suggesting that this close association appears to be independent of amyloid status and tracer.[30–35] Together, these observations suggest that a "dual-phase" approach of Aβ PET imaging, encompassing both early (first few minutes) and late (≈ 90–110 minutes) phase scanning, could provide complementary information about both pathological protein burden and patterns of brain perfusion/metabolism within the same scanning session. However, this hypothesis has not been investigated across a spectrum of cognitive dysfunction in a group in which amyloid pathology is not generally considered a major contributor to the phenotype.[29–32,36] This latter point is important as the early-phase scan may be of greatest clinical utility when the late-phase scan is amyloid negative.

After AD, Parkinson's disease (PD) is the second most prevalent neurodegenerative disorder worldwide.[37] Although motor manifestations traditionally characterize PD, cognitive impairment is common and is distributed across a spectrum from normal cognition (PD-N) to mild cognitive impairment (PD-MCI) to dementia (PDD).[38,39] Importantly, Aβ does not appear to be the main driver of the processes leading to dementia in PD.[40] In PD, progressive cognitive decline is consistently associated with reduced brain metabolism and perfusion, with many studies reporting similar patterns of hypometabolism/perfusion in predominantly posterior and prefrontal regions associated with increasing cognitive impairment.[26,41–44] Thus, PD serves to test the utility of early-phase Aβ PET, as cognitive impairment occurs across a spectrum, is not specifically associated with underlying brain amyloid status, and has clear patterns of altered metabolism and perfusion associated with cognitive decline.

Here, in a group of cognitively well-characterized PD participants ranging from normal cognition to dementia who had undergone dual-phase Aβ PET imaging and ASL MRI perfusion imaging, we investigated the utility of early-phase ^{18}F-florbetaben Aβ PET (eFBB) uptake as

RESEARCH IN CONTEXT

1. **Systematic Review**: Early-phase amyloid beta (Aβ) positron emission tomography (PET) is an emerging imaging modality with the potential to increase the efficiency of diagnostic tools in neurodegenerative disorders. The authors reviewed the current literature on this modality using traditional databases (PubMed), meeting abstracts, and presentations and hypothesized that early-phase Aβ PET may serve as a surrogate measure for perfusion, irrespective of amyloid pathology.
2. **Interpretation**: The current study showed that the early-phase PET uptake pattern is consistent with hypometabolic patterns associated with cognitive decline in PD. These patterns are consistent when accounting for late-phase Aβ status. Thus, early-phase PET may assess neurodegeneration associated with cognitive status.
3. **Future Directions**: Incorporating early-phase Aβ PET into routine clinical use may provide additional and complementary information about the state of the brain, in addition to the late-phase assessment of Aβ burden. The findings also suggest early-phase PET as an indicator of cognitive ability in neurodegenerative disorders and future prospective studies of cognitive decline.

a surrogate marker of cerebral perfusion/metabolism changes associated with cognitive status. We hypothesized that the association between eFBB uptake and cognitive status would mirror patterns of hypometabolism and hypoperfusion previously described in PD literature, irrespective of Aβ status, and eFBB uptake would positively correlate with a direct measure of cerebral perfusion: ASL MRI. Finally, we investigated the utility of eFBB uptake to distinguish PD participants across the cognitive spectrum (PD-N, PD-MCI, PDD).

2 | METHODS

A convenience sample of 118 PD patients meeting the UK Parkinson's Disease Society's criteria for idiopathic PD was recruited from volunteers at the Movement Disorders Clinic at the New Zealand Brain Research Institute, Christchurch, New Zealand.[45,46] Exclusion criteria included atypical Parkinsonism, prior learning disabilities, and a previous history of neurological conditions including moderate-to-severe head injury, vascular dementia, stroke, and major psychiatric or medical illnesses within the past 6 months. Additional neuroimaging screening (R.J.K.) excluded three participants from the final cohort, two with multifocal infarcts and one with partial extravasation of the bolus injection into soft tissue, leaving 115 participants for analysis. The participants have been previously described in Melzer et al.[40]

Participants completed early- and late-phase ^{18}F-FBB PET imaging, MRI scanning, and neuropsychological assessments. All participants provided written informed consent, with additional consent from a significant other when appropriate. The regional ethics committee of the New Zealand Ministry of Health (No. URB/09/08/037) approved the study.

2.1 | Neuropsychological assessment and cognitive diagnostic criteria

Extensive neuropsychological assessment across five cognitive domains was performed (attention and working memory, executive function, memory, visuospatial/visuoperceptual function, and language), consistent with Movement Disorders Society (MDS) Task Force Level II criteria.[47,48] For each domain, standardized scores from constituent neuropsychological tests were averaged to provide individual cognitive domain scores. Global cognitive performance for each participant was then expressed as an aggregate *z* score by averaging four domain scores excluding language (cognitive *z* score). Participants also completed the Montreal Cognitive Assessment (MoCA). All assessments (neuropsychological and imaging) were performed with patients on their usual dopaminergic medications.

PDD and PD-MCI were defined using established MDS criteria. PDD status required significant cognitive impairments (2 standard deviation [SD] below normative data) in at least two of the five cognitive domains, with evidence of significant impairments in everyday function not attributed to motor impairments.[45] PD-MCI cases required scores of 1.5 SD or more below normative data on at least two measures within a single cognitive domain, without significant impairments in activities of daily living, as verified by an interview with a significant other.[47,49] All remaining participants were classified as PD-N.

2.2 | Image data acquisition

2.2.1 | Positron emission tomography

eFBB was manufactured in Melbourne, Australia, by Cyclotek Pty Ltd and transported by airfreight to Christchurch, New Zealand, with sufficient radioactivity for three participant doses (after ≈ three half-lives in transit). After receiving an intravenous injection of 300 MBq ± 20% FBB, participants were scanned in "list mode" on a GE Discovery 690 PET/CT scanner (GE Healthcare). Early-phase images were reconstructed from 0 to 10 minutes and late-phase images from 90 to 110 minutes post-injection, using an iterative time-of-flight plus SharpIR algorithm. Standardized uptake value (SUV), the decay-corrected brain radioactivity concentration normalized for injected dose and body weight, was calculated at each voxel. A low-dose computed tomography (CT) scan was acquired immediately prior to PET scanning for attenuation correction. The voxel size in the reconstructed PET image was $1.2 \times 1.2 \times 3.2$ mm^3.

2.2.2 | Magnetic resonance imaging

MR images were acquired on a 3T GE HDxt scanner with an eight-channel head coil (GE Healthcare). A volumetric T1-weighted (inversion-prepared spoiled gradient echo [SPGR], echo time/repetition time = 2.8/6.6 ms, inversion time = 400 ms, flip angle 15°, acquisition matrix = 256 × 256 × 170, field of view = 250 mm, slice thickness = 1 mm) scan was acquired to facilitate spatial normalization of FBB PET images. Additional T2-weighted and T2 fluid-attenuated inversion recovery (FLAIR) images were acquired for a clinical read. PET and MRI scans were acquired, on average, 44.2 ± 57 days apart.

2.2.3 | Arterial spin labeling—perfusion MRI

A stack of spiral, fast spin echo acquired images, prepared using pseudo-continuous ASL (PCASL) and background suppression, was used to measure whole-brain quantitative perfusion (repetition time = 6 seconds, echo spacing = 9.2 ms, post-labeling delay = 1.525 seconds, labeling duration = 1.5 seconds, eight interleaved spiral arms with 512 samples at 62.5 kHz bandwidth and 30 phase-encoded 5 mm thick slices, NEX = 5, total scan time = 6 minutes 46 seconds, units: mL/100 g/minute). The images were acquired with the participant at rest with their eyes closed. ASL MRI from 8 of the 115 individuals was not available due to poor signal labeling (n = 2), delayed bolus arrival (n = 4), spiral artefact (n = 1), and ASL not being acquired (n = 1). Of these, five were PDD, two PD-MCI, and one PD-N. Thus, eFBB PET and ASL MRI from the remaining 107 participants were used for cross-modality comparisons.

2.3 | Image processing

2.3.1 | Structural MRI data

T1-weighted structural images were processed with CAT12 (r934) in SPM (v6685) via MATLAB 9.0.0 (R2016a). Images were bias-corrected, spatially normalized via DARTEL (using the Montreal Neurological Institute [MNI]-registered template provided in CAT12), modulated to compensate for the effect of spatial normalization, and classified into gray matter (GM), white matter (WM), and CSF, all within the same generative model.[50]

2.3.2 | Early-phase ^{18}F-FBB data

Early-phase PET images (0–10 minutes) were co-registered to subject T1-weighted images and normalized to MNI space using MRI-derived deformation fields. Individual SUV ratio (SUVR) images were calculated by scaling to the mean signal in the Centiloid project whole cerebellum reference region of interest, and the images were smoothed using a 8 mm isotropic Gaussian kernel for whole-brain analysis.[51]

2.3.3 | Arterial spin labeling data

The scanner-generated quantified cerebral blood flow (CBF) images were co-registered to subject T1-weighted structural images, normalized to MNI space using MRI-derived deformation fields, and smoothed (8 mm). Mean cortical CBF was extracted from the standard Centiloid cortical region.

2.4 | Analysis approaches

2.4.1 | Classification of amyloid status

A neuroradiologist (R.J.K., with both in-person and e-training, and 10 years' experience reporting FBB scans), blinded to cognitive status, rated each late-phase scan as amyloid positive or negative based on the assessment of FBB uptake in GM versus WM in the lateral, temporal, frontal, posterior cingulate/precuneus, and parietal lobes (in accordance with NeuraCeq™ guidelines: https://www.accessdata.fda.gov/drugsatfda_docs/label/2014/204677s000lbl.pdf).[52]

Measures of Aβ status and the role of Aβ in PD cognitive ability from this cohort have been previously reported by Melzer et al.[40]

2.4.2 | Whole-brain voxel-wise analysis

To determine the association between eFBB SUVR and global cognitive ability (cognitive z score), a voxel-wise multiple linear regression using a permutation-based inference tool for non-parametric thresholding was conducted with age, sex, and years of education as covariates (randomise in FSL).[53] Additional analyses were conducted (1) with late-phase Aβ status as a covariate (in addition to age and years of education) and (2) with amyloid-negative–only individuals (n = 94) to determine the impact of Aβ on the relationship between early-phase uptake and cognitive ability. All voxel-wise analyses were corrected for multiple comparisons (family wise error correction using threshold-free cluster enhancement [TFCE], $P < 0.05$).[54] These regression models were also repeated for ASL MRI CBF images.

2.4.3 | Region of interest analysis across modalities

To compare eFBB to an established cerebral perfusion measure (ASL), we extracted average SUVR and perfusion from all cortical and subcortical ROIs defined by the Automated Anatomical Labeling (AAL3) atlas. Pearson correlation coefficients within each ROI were then calculated to assess the association between eFBB SUVR and ASL-derived CBF. P values were adjusted for multiple comparisons using false discovery rate (FDR) in R (v4.3.0).

2.4.4 | Receiver operating characteristics

We conducted a receiver operating characteristic (ROC) analysis to assess the diagnostic performance of eFBB GM SUVR in distinguishing among different cognitive groups. We used the AAL3 atlas to generate cortical masks of pre-specified brain regions in which a recent meta-analysis identified associations between hypometabolism and cognitive impairment in PD (inferior parietal cortex and the caudate nucleus).[55] We extracted average eFBB SUVR from these regions and performed a ROC analysis using the pROC package in R (v4.3.0) to provide the area under the curve (AUC), sensitivity, and specificity. Statistical significance was assessed with a non-parametric bootstrap method with 1000 resamples to estimate 95% confidence intervals (CI).

3 | RESULTS

3.1 | Demographics

Table 1 summarizes the demographic and clinical information for the PD participants with group comparisons using analysis of variance. Twenty-one of 115 (18%) were amyloid positive. Table 2 provides group comparisons among the different cognitive groups with post hoc Tukey analysis. While PD-N and PD-MCI showed no group differences in age and Unified Parkinson's Disease Rating Scale (UPDRS) Part III scores, PD-MCI showed statistically significantly lower MoCA, and cognitive *z* scores than the PD-N cohort. Meanwhile, the PDD group were significantly older, with poorer MoCA, UPDRS Part III, and cognitive *z* score than the other two groups. The relationship between clinical amyloid status and the individual Centiloid values is presented in Figure S1 in supporting information.

3.2 | Early-phase FBB uptake is associated with cognitive performance in PD

There were significant associations between early-phase FBB SUVR and cognitive *z* score in several cortical and subcortical areas (TFCE-corrected, $P < 0.05$, Figure 1A), including parieto-occipital regions (precuneus, cuneus, posterior cingulate, inferior parietal cortex, and lateral occipital cortices), middle and inferior temporal gyri, left prefrontal cortex, and bilateral thalami. These regions were largely unchanged and still significant after adding Aβ status (positive/negative—from the late-phase scan) as a covariate (Figure S2 in supporting information). Notably, this pattern of association is strikingly similar to previous work examining the relationship between brain metabolism and cognitive impairment in PD.[53–55] The results from the amyloid-negative only sample largely mirrored the results produced when including all participants but were more spatially restricted and did not include the thalamus (Figure S3 in supporting information). However, the association between early-phase uptake in the precuneus, parietooccipital, and occipito-temporal regions, and the global cognitive score remained significant. The difference in results between the two analyses may be attributable to a reduction in power due to a smaller sample size, a limited variance present in the amyloid-negative group, or the association may not be as strong in the amyloid-negative group, among other possibilities.

3.3 | Early-phase FBB uptake is associated with ASL MRI measures of perfusion

Early-phase PET and ASL MRI modalities showed correlations across widespread brain regions (Figure 2). These relationships were evident in both cortical and subcortical regions. These included parietal regions (inferior parietal, angular gyri, supramarginal gyri, and precuneus [$r = 0.27–0.49$, corrected $P < 0.005$]), prefrontal cortical regions ($r = 0.36–0.47$, corrected $P < 0.005$), hippocampus, and subcortical regions including thalamus, caudate, and lentiform nucleus ($r = 0.15–0.41$, corrected $P < 0.005$).

3.4 | Diagnostic value of early-phase FBB uptake

Finally, we investigated the utility of eFBB in distinguishing PD participants with dementia from those with normal cognition. The PDD cohort's mean GM eFBB uptake was significantly lower than the PD-N participants (Figure 3A, Mann–Whitney test, $U = 307$, $P = 0.0003$). ROC analysis using mean GM eFBB uptake showed good discrimination between PDD and PD-N, yielding a specificity of 81.3% and a sensitivity of 74.0% (AUC [95% CI] = 0.83 [0.71, 0.96]; Figure 3C). However, a priori, we used a GM mask derived from regions where FDG-PET metabolism correlated with cognitive ability in PD per a recent meta-analysis.[55] Using this mask for ROC analysis, eFBB uptake showed strong discriminative ability between PD-N and PDD with a specificity of 90.9% and a sensitivity of 81.8% (AUC [95% CI] = 0.91 [0.80, 100]; Figure 3D). eFBB uptake in this mask also discriminated PDD reasonably from PD-MCI cohorts (Figure 3E, specificity: 67.6%, sensitivity: 81.8%, AUC [95% CI] = 0.78 [0.65, 0.92]) but showed poor ability to discriminate between PD-N and PD-MCI groups (Figure 3F). For comparison, Figure 3B dispalys the mean GM CBF across cognitive groups.

4 | DISCUSSION

Emerging work has suggested that early-phase Aβ PET imaging may provide complementary information to the clinically established late-phase Aβ PET assessment of amyloid status. In this study, we evaluated the utility of early-phase PET imaging as a metabolism/perfusion surrogate using a large cohort of people with PD spanning a spectrum of cognitive performance from normal to dementia using Aβ PET tracer eFBB. eFBB uptake reproduced the previously well-established patterns of altered perfusion and metabolism associated with cognitive impairment in PD. Importantly, this relationship between uptake and cognitive ability was independent of individual amyloid status.

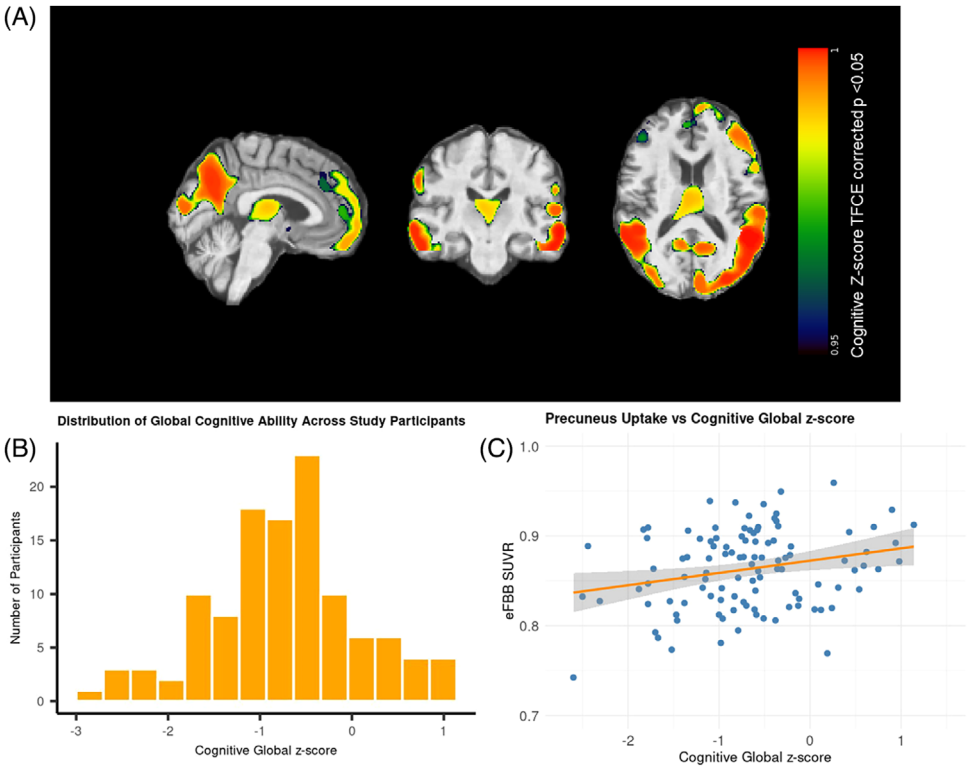

FIGURE 1 Association between eFBB uptake and cognitive impairment in PD; (A) indicates voxels with a significant positive association between early-phase FBB SUVR and global cognitive score (age, sex, and years of education as covariates; color bar corresponding to 1-p, corrected $P < 0.05$). B, The distribution of study participants across a cognitive spectrum, measured by global cognitive *z* score as described in the Methods section. C, The association between early-phase FBB SUVR and cognitive ability in a representative region (precuneus). CogZ, cognitive *z* score; eFBB, early-phase florbetaben; PDD, Parkinson's disease dementia; PD-MCI, Parkinson's disease with mild cognitive impairment; PD-N, cognitively normal Parkinson's disease; SUVR, standardized uptake value ratio; TFCE, threshold-free cluster enhancement

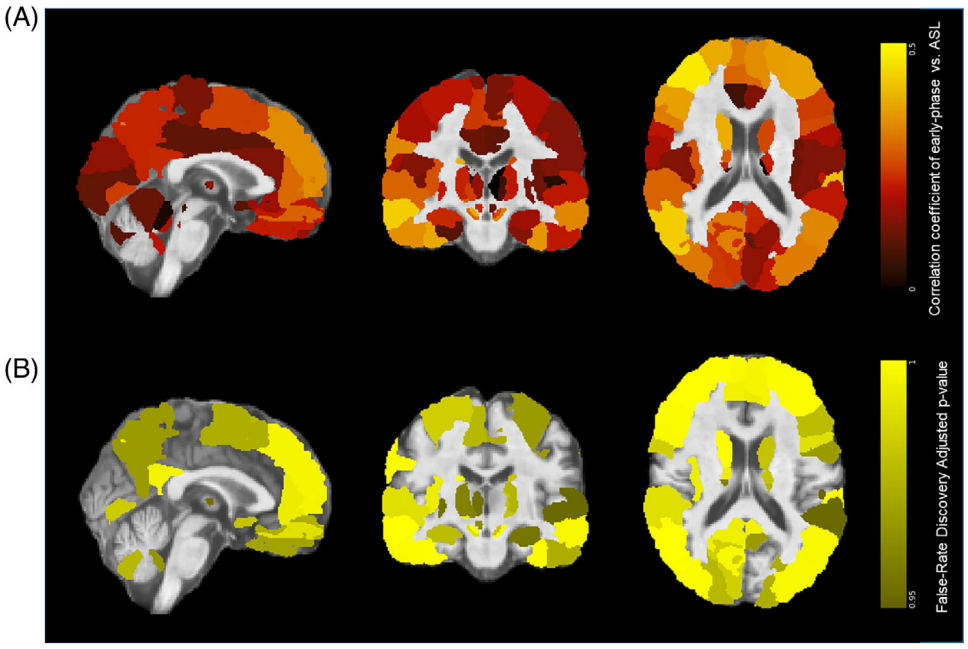

FIGURE 2 Correlation map between early-phase FBB SUVR and ASL MRI measured CBF in regions defined by AAL3. A, The magnitude of the correlation as defined by the Pearson correlation coefficient. B, Significantly correlated regions adjusted for false discovery rate (color bar corresponding to 1-p). AAL, Automated Anatomical labeling; ASL, arterial spin labeling; CBF, cerebral blood flow; FBB, florbetaben; MRI, magnetic resonance imaging; SUVR, standardized uptake value ratio

TABLE 1 Demographics and cognitive and clinical metrics.

Diagnosis	PD-N	PD-MCI	PDD	Group comparison
Total	23	76	16	
Female no. (%)	8 (35)	18 (24)	3 (19)	$\chi 2 = 1.5$ $P = 0.46$
Age (years)	70 (6)	72 (6)	77 (6)	$F(2,112) = 6.6$ $P = 0.002$
Education (years)	12 (2)	13 (3)	12 (2)	$F(2,112) = 0.3$ $P = 0.76$
PD symptom duration (years)	7.4 (5)	7.3 (4)	8.5 (5)	$F(2,112) = 0.3$ $P = 0.76$
UPDRS Part III	38 (15)	39 (13)	53 (8.8)	$F(2,102) = 4.6$ $P = 0.01$
MoCA	26 (2)	23 (3)	16 (5)	$F(2,112) = 45.1$ $P < 0.001$
Cognitive *z* score	0.28 (0.48)	−0.81 (0.53)	−1.89 (0.57)[a]	$F(2,112) = 83.0$ $P < 0.001$
Attention score	−0.034 (0.51)	−0.89 (0.58)	−1.87 (0.67)[a]	$F(2,106) = 38.7$ $P < 0.001$
Executive function score	0.37 (0.60)	−0.92 (0.73)	−1.85 (0.47)[a]	$F(2,106) = 46.3$ $P < 0.001$
Visuospatial/perception score	0.27 (0.58)	0.61 (0.73)	−1.69 (0.65)[a]	$F(2,106) = 29.0$ $P < 0.001$
Memory domain score	0.52 (0.86)	−0.82 (0.85)	−1.82 (0.67)	$F(2,112) = 40.0$ $P < 0.001$
Language score	0.08 (0.52)	−0.43 (0.60)	−1.17 (0.72)[a]	$F(2,106) = 15.6$ $P < 0.001$
Dose (MBq)	294 (20)	300 (16)	290 (27)	$F(2,112) = 2.4$ $P = 0.09$
Aβ positivity (%)	4 (17)	11 (14)	6 (38)	$\chi 2 = 4.7$ $P = 0.10$

Note: Values are mean (standard deviation) unless specified. Analysis of variance was used to assess age, education, symptom duration, UDPRS, MoCA, cognitive *z* score, domains, and injected dose, while $\chi 2$ tests were used to assess sex distribution and Aβ positivity. Cognitive *z* scores were calculated as specified in the Methods section.

Abbreviations: Aβ, amyloid beta; MBq, megabecquerel; MoCA, Montreal Cognitive Assessment; PDD, Parkinson's disease dementia; PD-MCI: Parkinson's disease with mild cognitive impairment; PD-N, cognitively normal Parkinson's disease.

[a]Cognitive z scores for six PDD participants were imputed from restricted neuropsychological data due to their inability to complete the full cognitive assessment.

Furthermore, eFBB was significantly correlated with a direct measure of cerebral perfusion (measured with ASL MRI) across both cortical and subcortical regions. Finally, early-phase uptake distinguished PD patients with normal cognition from those with dementia with relatively high accuracy. Together, these results provide evidence that eFBB may be a reliable surrogate for cerebral metabolism and perfusion, opening clear opportunities for incorporating it into diagnostic and management pathways for people with cognitive impairment in combination with late-phase amyloid PET imaging.

The current study allowed us to examine the relationship between early-phase uptake and cognitive impairment in PD, providing an informative example of predominantly Aβ-negative neurodegeneration. The pattern of brain hypometabolism and hypoperfusion associated with cognitive impairment and dementia in PD consistently includes parieto-occipital and frontal hypometabolism across various ^{18}F-FDG PET studies, which we were able to reproduce with eFBB, supporting the idea that early-phase Aβ PET can serve as a surrogate of ^{18}F-FDG PET in assessing brain metabolism.[56–58] Knowledge about underlying brain metabolism, in addition to amyloid status, may also provide important prognostic information in people with cognitive impairment secondary to AD (i.e., in which late-phase amyloid imaging is positive).[21,59] As such, the additional information provided by dual-phase Aβ PET imaging holds significant promise for streamlining patient diagnostic and management pathways.

To further assess the real-world potential of eFBB to quantify neurodegeneration through metabolism and/or perfusion, we directly compared eFBB uptake to ASL MRI, an established measure of cerebral perfusion. Like metabolism, a posterior pattern of hypoperfusion is a

TABLE 2 Group comparisons.

Group differences	PD-N versus PD-MCI	PD-N versus PDD	PD-MCI versus PDD
Age (years)	−2.2 ($P = 0.24$)	**−6.8 ($P = 0.001$)**	**−4.6 ($P = 0.013$)**
MoCA	**3.4 ($P < 0.001$)**	**9.86 ($P < 0.001$)**	**6.46 ($P < 0.001$)**
UPDRS Part III	−1.3 ($P = 0.92$)	**−15.1 ($P = 0.015$)**	**−13.8 ($P = 0.013$)**
Cognitive *z* score	**1.1 ($P < 0.001$)**	**2.2 ($P < 0.001$)**	**1.1 ($P < 0.001$)**
Attention score	**0.86 ($P < 0.001$)**	**1.8 ($P < 0.001$)**	**0.98 ($P < 0.001$)**
Executive function score	**1.3 ($P < 0.001$)**	**2.2 ($P < 0.001$)**	**0.93 ($P < 0.001$)**
Visuospatial/perception score	**0.87 ($P < 0.001$)**	**2.0 ($P < 0.001$)**	**1.1 ($P < 0.001$)**
Memory domain score	**1.3 ($P < 0.001$)**	**2.3 ($P < 0.001$)**	**1.0 ($P < 0.001$)**
Language score	**0.5 ($P = 0.0015$)**	**1.3 ($P < 0.001$)**	**0.7 ($P < 0.001$)**

Note: Group comparisons from Table 1 were further analyzed using the Tukey test. Statistically significant comparisons are highlighted in bold.
Abbreviations: Aβ, amyloid beta; MBq, megabecquerel; MoCA, Montreal Cognitive Assessment; PDD, Parkinson's disease dementia; PD-MCI: Parkinson's disease with mild cognitive impairment; PD-N, Cognitively normal Parkinson's disease; UPDRS, Unified Parkinson's Disease Rating Scale.

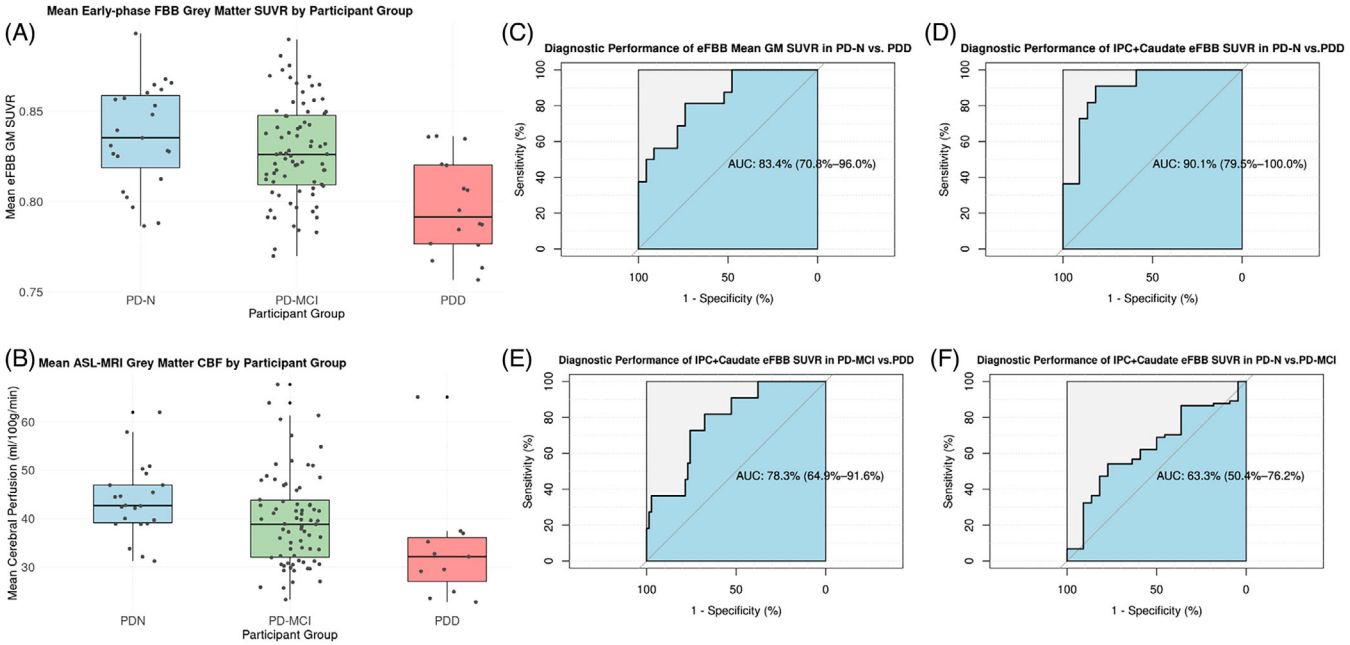

FIGURE 3 The clinical utility of early-phase FBB uptake in distinguishing cognitive groups. A, The mean GM eFBB uptake between cognitive groups. Uptake decreased across the cognitive categories from normal to dementia, with the PD-MCI group showing the biggest within-group variation. B, Mean GM CBF (ASL) across cognitive groups, following the pattern observed with early-phase FBB. C, ROC analysis for eFBB SUVR ability to distinguish dementia presence using Mean GM SUVR. (D)–(F). Meta-analysis-based ROC for distinguishing (D) PDD from PD-N, (E) PDD from PD-MCI and (F) PD-MCI from PD-N.[52] ASL, arterial spin labeling; AUC, area under the curve (95% confidence interval); CBF, cerebral blood flow; eFBB, early-phase florbetaben; GM, gray matter; IPC, inferior parietal cortex (angular, supramarginal and inferior parietal gyrus); PDD, Parkinson's disease dementia; PD-MCI, Parkinson's disease with mild cognitive impairment; PD-N, cognitively normal Parkinson's disease; ROC, receiver operating characteristic; SUVR, standardized uptake value ratio

well-documented feature of PD, with additional deficits in the dorsolateral prefrontal and temporal cortices and subcortically in the thalamus and the caudate.[26,60–64] Our findings revealed widespread correlations between eFBB PET uptake and ASL MRI measures of CBF, encompassing both cortical and subcortical regions. The strongest correlations were observed in the dorsolateral prefrontal cortex, parieto-occipital, and temporal regions. Furthermore, we observed a decline in global mean GM uptake of eFBB and mean GM CBF from ASL MRI across cognitive stages despite a considerable variation in the PD-MCI subgroup, indicating similarities between the two methods. However, the two measures were not perfectly correlated, and some cortical and subcortical regions only showed modest correlations between the two modalities. It is possible that early phase may more closely mirror metabolism than perfusion, as previous early-phase PET comparisons

have shown higher correlations with FDG PET than ASL MRI.[31,65] In addition, differences in test–retest reliability between the two techniques may contribute to some areas of lower correlations.[66,67] Although unlikely to be a significant driver of the differences, the PET and MRI scans were acquired on different days (on average, 44.2 ± 57 days apart).

Disease-specific patterns of abnormal metabolism, measured via FDG PET, have been described across neurodegenerative disorders, including idiopathic PD, AD, Huntington's disease, multiple system atrophy, and progressive supranuclear palsy.[41,68] However, reproducing these patterns derived via early-phase FBB PET is an emerging field. With amyloid tracer AV45, Vanhoutte et al. identified a pattern of early-phase deficits across the AD spectrum (high amyloid with MCI or dementia).[33] Relative to low-amyloid elderly controls, these individuals exhibited lowered uptake in the lateral posterior parietal, precuneus, and posterior cingulate. In a similar study, amnestic MCI exhibited slightly less early-phase PiB uptake in the posterior cingulate, while AD showed significantly lowered uptake in the posterior cingulate, posterior (lateral) parietal cortex, and both medial and lateral temporal lobes compared to healthy controls.[30] Our results within a PD cohort showed an association between eFBB and cognitive ability in regions overlapping with AD-related hypoperfusion. However, we also observed associations within the frontal and occipital lobes and a lack of explicit medial temporal lobe hypoperfusion. Thus, the high correlation between early-phase Aβ PET and FDG PET, the robustness of FDG pattern across conditions, and the current results showing consistencies with PD patterns distinct from AD-defined patterns indicate that early-phase amyloid PET is a promising technique for identifying disease-specific patterns of abnormal perfusion.

There is a clear need for robust biomarkers to facilitate accurate and timely diagnoses in individuals with cognitive impairment. This is exemplified by the emergence of molecular biomarkers for AD, including late-phase amyloid PET imaging.[12] However, in many clinical scenarios, knowledge of a person's amyloid status alone is insufficient to confidently diagnose the cause of their cognitive impairment, and information about the presence and the patterns of neurodegeneration can provide crucial complementary information for improving diagnostic accuracy and patient outcomes.[21,69] Biomarkers in routine clinical practice should also consider factors such as cost effectiveness, patient burden, time, and radiotracer exposure that—for example, multiple PET imaging scans—would impose. In this setting, the opportunity of dual-phase Aβ PET imaging has emerged with the potential to acquire information on both Aβ burden and neurodegeneration within a single procedure. The early-phase PET modality bypasses the need for additional measurements such as an additional ^{18}F-FDG PET—streamlining diagnostic assessments and costs—and ultimately could translate into a faster, cheaper, and equally accurate diagnostic pathway for people experiencing cognitive difficulties. Recent studies investigating the relationship between early-phase Aβ PET and ^{18}F-FDG PET—the gold standard metabolic measurement—in the context of AD have demonstrated early-phase PET's ability to provide a similar (visually and quantitative) assessment of neuronal damage to that of FDG-PET.[29–32]

The additional information provided by the early-phase Aβ PET scan may prove most helpful in diagnosing cases in which the late-phase scan is negative. In such scenarios, the neurodegenerative differential diagnosis often includes disorders characterized by well-established patterns of perfusion and metabolism abnormalities (e.g., frontotemporal dementias, dementia with Lewy bodies, corticobasal syndrome).[70–72] Conversely, a normal early-phase Aβ PET scan could provide support for a primarily psychological cause of cognitive impairment, which is an important differential in people presenting with memory complaints.[73] Additionally, in those who are Aβ positive, amyloid SUVR shows a limited ability to predict future decline, whereas neurodegeneration measures may provide important information about disease trajectory and consequently inform both patient discussions and disease management strategies.[21,74] Moreover, early-phase imaging holds significant promise in the realm of therapeutic advancement. With increasing interest and investment in pharmaceutical and therapeutic interventions aimed at diminishing pathological protein levels, PET imaging is at its most prominent as a pivotal tool for confirming the presence of pathological protein burden and assessing the efficacy of treatments.[5,6] In this context, early-phase Aβ PET may aid in selecting appropriate patients and serve as an additional outcome measure for clinical trials aimed at disease modification. Finally, the concept of early-phase dynamics also has the potential to expand beyond Aβ PET imaging to other radiotracers, such as those targeting dopamine transporter or neurofibrillary tau, thus potentially aiding the evaluation of Parkinsonism, tauopathies, and other neurodegenerative disorders.[75–77]

In interpreting the results of this study, it is important to consider its potential limitations. ^{18}F-FDG PET imaging, long considered the gold standard for brain metabolism assessment, was not available as a direct comparison. However, we had a strong a priori knowledge about the metabolic patterns associated with cognitive decline in PD and a direct measure of cerebral perfusion (ASL MRI), which is tightly linked to underlying brain metabolism.[67,78,79] The study did not include a healthy control group, limiting the extension of these findings to those without any brain disorders. However, the inclusion of many people without cognitive impairment shows the utility of early-phase PET across a broad cognitive spectrum, while previous work has examined this modality in healthy individuals.[29,30] Further work should examine the predictive potential of early-phase PET by tracking cohorts longitudinally—focusing on individuals transitioning to dementia from normal cognition and MCI—to reveal early signs of risk related to regional or global early-phase uptake, as has been conducted in FDG PET studies.[73] This would be particularly relevant in those with MCI status—a particularly heterogeneous group in the context of PD.[79]

While the current study used the Centiloid whole cerebellum as the reference region SUVR calculation, reference region selection for neurodegenerative disorders is an ongoing topic of discussion in the PET imaging field. Studies have explored various reference regions for normalizing late- and early-phase uptake (e.g., whole cerebellum, cerebellar cortex, pons, global mean, WM, mixed regions).[31–33] Of these, the cerebellum has low susceptibility to age-related atrophy, minimal changes in metabolism, and CBF, and, from an amyloid perspective,

demonstrates low or absent amyloid plaque burden. However, studies have reported a lowered or no difference in cerebellar perfusion in PD compared to controls or relative increases in cerebellar metabolism associated with cognitive ability in PD.[80–82] Systematic decreases or increases in the reference region will lead to artefactual SUVR increases and decreases, respectively.[83] While the whole cerebellum was suitable for the current study, future work may evaluate several reference regions, such as a combined cerebellum and pons.[33] We used SUVR for both early- and late-phase acquisitions because of its simplicity and feasibility in PET imaging. In addition to low variability, SUVR offers reduced patient burden compared to quantitative measures, a considerable advantage for our PD cohort due to their motor and cognitive symptoms. However, its accuracy relies on establishing true equilibrium, which remains susceptible to bias due to tracer clearance effects and, for clinical cohorts, may be affected by regional perfusion differences and disruptions in the blood–brain barrier. As such, while the study accounted for the influence of late-phase amyloid on the early-phase SUVR, the inverse of whether perfusion alterations may affect late-phase amyloid quantification was not directly explored in this work; future studies may benefit from investigating this relationship quantitatively.

The current study suggests the ability of early-phase Aβ PET imaging to provide a clinically relevant surrogate measure of brain metabolism/perfusion in a large cohort of people with PD ranging across the cognitive spectrum, independent of brain amyloid status. It provides evidence for early-phase PET imaging as a surrogate for validated neurodegeneration measures. Overall, it demonstrates the exciting potential of dual-phase (early and late) Aβ PET imaging to streamline diagnostic pathways for people with cognitive impairment as the field moves into an exciting new area of potential disease modification.

ACKNOWLEDGMENTS

We thank all our participants and their families for their long-standing support and the New Zealand Brain Research Institute staff and students. The study was funded by the Health Research Council of New Zealand (14-440, 17-039), Neurological Foundation, Rangahau Roro Aotearoa, Canterbury Medical Research Foundation (14/04), New Zealand Brain Research Institute, Lottery Health Research (72620), University of Otago, and the Orr family.

Open access publishing facilitated by University of Otago, as part of the Wiley - University of Otago agreement via the Council of Australian University Librarians.

CONFLICT OF INTEREST STATEMENT

The authors declare no conflicts of interest related to this research. The principal author confirms that all authors have read the manuscript, and the paper has not previously been published or is under consideration at another journal. The authors take full responsibility for the data, analyses, and interpretation, and the conduct of the research, and have full access to all the data and the right to publish it. All authors have agreed to the conditions noted on the authorship agreement form.

CONSENT STATEMENT

All human participants in the current study provided informed consent.

ORCID

Tracy R. Melzer https://orcid.org/0000-0003-0621-212X

REFERENCES

1. Shah H, Albanese E, Duggan C, et al. Research priorities to reduce the global burden of dementia by 2025. *Lancet Neurol*. 2016;15(12):1285-1294. doi:10.1016/S1474-4422(16)30235-6
2. Brodtmann A, Darby D, Oboudiyat C, et al. Assessing preparedness for Alzheimer disease-modifying therapies in Australasian health care systems. *Med J Aust*. 2023;218(6):247-249. doi:10.5694/mja2.51880
3. Dubois B, Padovani A, Scheltens P, Rossi A, Dell'Agnello G. Timely diagnosis for Alzheimer's disease: a literature review on benefits and challenges. *JAD*. 2015;49(3):617-631. doi:10.3233/JAD-150692
4. Robinson L, Tang E, Taylor JP. Dementia: timely diagnosis and early intervention. *BMJ*. 2015;350:h3029-h3029. doi:10.1136/bmj.h3029
5. Van Dyck CH, Swanson CJ, Aisen P, et al. Lecanemab in early Alzheimer's disease. *N Engl J Med*. 2023;388(1):9-21. doi:10.1056/NEJMoa2212948
6. Reardon S. Alzheimer's drug donanemab: what promising trial means for treatments. *Nature*. 2023;617(7960):232-233. doi:10.1038/d41586-023-01537-5
7. Thal LJ, Kantarci K, Reiman EM, et al. The role of biomarkers in clinical trials for Alzheimer disease. *Alzheimer Dis Assoc Disord*. 2006;20(1):6-15. doi:10.1097/01.wad.0000191420.61260.a8
8. Bayer AJ. The role of biomarkers and imaging in the clinical diagnosis of dementia. *Age Ageing*. 2018;47(5):641-643. doi:10.1093/ageing/afy004
9. Cummings J. The role of biomarkers in Alzheimer's disease drug development. In: Guest PC, ed. *Reviews on Biomarker Studies in Psychiatric and Neurodegenerative Disorders*. Springer International Publishing; 1118:29-61. doi:10.1007/978-3-030-05542-4_2. Advances in Experimental Medicine and Biology.
10. Blennow K, Hampel H, Weiner M, Zetterberg H. Cerebrospinal fluid and plasma biomarkers in Alzheimer disease. *Nat Rev Neurol*. 2010;6(3):131-144. doi:10.1038/nrneurol.2010.4
11. Molinuevo JL, Blennow K, Dubois B, et al. The clinical use of cerebrospinal fluid biomarker testing for Alzheimer's disease diagnosis: a consensus paper from the Alzheimer's biomarkers standardization initiative. *Alzheimers Dement*. 2014;10(6):808-817. doi:10.1016/j.jalz.2014.03.003
12. Johnson KA, Minoshima S, Bohnen NI, et al. Update on appropriate use criteria for amyloid PET imaging: dementia experts, mild cognitive impairment, and education. *J Nucl Med*. 2013;54(7):1011-1013. doi:10.2967/jnumed.113.127068
13. Lee YS, Youn H, Jeong HG, et al. Cost-effectiveness of using amyloid positron emission tomography in individuals with mild cognitive impairment. *Cost Eff Resour Alloc*. 2021;19(1):50. doi:10.1186/s12962-021-00300-9
14. Engler H, Santillo AF, Wang SX, et al. In vivo amyloid imaging with PET in frontotemporal dementia. *Eur J Nucl Med Mol Imaging*. 2008;35(1):100-106. doi:10.1007/s00259-007-0523-1
15. Farid K, Hong YT, Aigbirhio FI, et al. Early-phase 11C-PiB PET in amyloid angiopathy-related symptomatic cerebral hemorrhage: potential diagnostic value? *PLoS ONE*. 2015;10(10):e0139926. doi:10.1371/journal.pone.0139926
16. Parmera JB, Coutinho AM, Aranha MR, et al. FDG-PET Patterns predict amyloid deposition and clinical profile in corticobasal syndrome. *Mov Disord*. 2021;36(3):651-661. doi:10.1002/mds.28373

17. Rodrigue KM, Kennedy KM, Park DC. Beta-amyloid deposition and the aging brain. *Neuropsychol Rev*. 2009;19(4):436-450. doi:10.1007/s11065-009-9118-x
18. Edison P, Rowe CC, Rinne JO, et al. Amyloid load in Parkinson's disease dementia and Lewy body dementia measured with [11C]PIB positron emission tomography. *J Neurol Neurosurg Psychiatry*. 2008;79(12):1331-1338. doi:10.1136/jnnp.2007.127878
19. Kantarci K, Lowe VJ, Boeve BF, et al. AV-1451 tau and β-amyloid positron emission tomography imaging in dementia with Lewy bodies: tau and Amyloid PET in DLB. *Ann Neurol*. 2017;81(1):58-67. doi:10.1002/ana.24825
20. Sengupta U, Kayed R. Amyloid β, Tau, and α-Synuclein aggregates in the pathogenesis, prognosis, and therapeutics for neurodegenerative diseases. *Prog. Neurobiol*. 2022;214:102270. doi:10.1016/j.pneurobio.2022.102270
21. Chételat G, Arbizu J, Barthel H, et al. Amyloid-PET and 18F-FDG-PET in the diagnostic investigation of Alzheimer's disease and other dementias. *Lancet Neurol*. 2020;19(11):951-962. doi:10.1016/S1474-4422(20)30314-8
22. Dubois B, Feldman HH, Jacova C, et al. Advancing research diagnostic criteria for Alzheimer's disease: the IWG-2 criteria. *Lancet Neurol*. 2014;13(6):614-629. doi:10.1016/S1474-4422(14)70090-0
23. Nestor PJ, Altomare D, Festari C et al, for the EANM-EAN Task Force for the Prescription of FDG-PET for Dementing Neurodegenerative Disorders. Clinical utility of FDG-PET for the differential diagnosis among the main forms of dementia. *Eur J Nucl Med Mol Imaging*. 2018;45(9):1509-1525. doi:10.1007/s00259-018-4035-y
24. Silverman DHS. Brain 18F-FDG PET in the Diagnosis of Neurodegenerative Dementias: Comparison with Perfusion SPECT and with Clinical Evaluations Lacking Nuclear Imaging. *J Nucl Med*. 2004;45(4):594-607.
25. Davison CM, O'Brien JT. A comparison of FDG-PET and blood flow SPECT in the diagnosis of neurodegenerative dementias: a systematic review. *Int J Geriatr Psychiatry*. 2014;29(6):551-561. doi:10.1002/gps.4036
26. Melzer TR, Watts R, MacAskill MR, et al. Arterial spin labelling reveals an abnormal cerebral perfusion pattern in Parkinson's disease. *Brain*. 2011;134(3):845-855. doi:10.1093/brain/awq377
27. Peterson EC, Wang Z, Britz G. Regulation of cerebral blood flow. *Int J Vasc*. 2011;2011:1-8. doi:10.1155/2011/823525
28. Claassen JAHR, Thijssen DHJ, Panerai RB, Faraci FM. Regulation of cerebral blood flow in humans: physiology and clinical implications of autoregulation. *Physiological Reviews*. 2021;101(4):1487-1559. doi:10.1152/physrev.00022.2020
29. Vanhoutte M, Landeau B, Sherif S, et al. Optimization of early-phase florbetapir as a surrogate of FDG-PET in ageing and Alzheimer's clinical syndrome: neuroimaging /New imaging methods. *Alzheimer Dementia*. 2020;16(S4). doi:10.1002/alz.040232
30. Bunai T, Kakimoto A, Yoshikawa E, Terada T, Ouchi Y. Biopathological significance of early-phase amyloid imaging in the spectrum of Alzheimer's Disease. *JAD*. 2019;69(2):529-538. doi:10.3233/JAD-181188
31. Daerr S, Brendel M, Zach C, et al. Evaluation of early-phase [18 F]-florbetaben PET acquisition in clinical routine cases. *NeuroImage: Clinical*. 2017;14:77-86. doi:10.1016/j.nicl.2016.10.005
32. Hsiao IT, Huang CC, Hsieh CJ, et al. Correlation of early-phase 18F-florbetapir (AV-45/Amyvid) PET images to FDG images: preliminary studies. *Eur J Nucl Med Mol Imaging*. 2012;39(4):613-620. doi:10.1007/s00259-011-2051-2
33. Vanhoutte M, Landeau B, Sherif S, et al. Evaluation of the early-phase [18F]AV45 PET as an optimal surrogate of [18F]FDG PET in ageing and Alzheimer's clinical syndrome. *NeuroImage: Clinical*. 2021;31:102750. doi:10.1016/j.nicl.2021.102750
34. Tiepolt S, Hesse S, Patt M, et al. Early [18F]florbetaben and [11C]PiB PET images are a surrogate biomarker of neuronal injury in Alzheimer's disease. *Eur J Nucl Med Mol Imaging*. 2016;43(9):1700-1709. doi:10.1007/s00259-016-3353-1
35. Boccalini C, Peretti DE, Ribaldi F, et al. Early-phase ^{18} F-Florbetapir and ^{18} F-flutemetamol images as proxies of brain metabolism in a memory clinic setting. *J Nucl Med*. 2023;64(2):266-273. doi:10.2967/jnumed.122.264256
36. Okazawa H, Ikawa M, Jung M, et al. Multimodal analysis using [11C]PiB-PET/MRI for functional evaluation of patients with Alzheimer's disease. *EJNMMI Res*. 2020;10(1):30. doi:10.1186/s13550-020-00619-z
37. Ou Z, Pan J, Tang S, et al. Global trends in the incidence, prevalence, and years lived with disability of Parkinson's Disease in 204 countries/territories from 1990 to 2019. *Front Public Health*. 2021;9:776847. doi:10.3389/fpubh.2021.776847
38. Poewe W, Seppi K, Tanner CM, et al. Parkinson disease. *Nat Rev Dis Primers*. 2017;3(1):17013. doi:10.1038/nrdp.2017.13
39. Hely MA, Reid WGJ, Adena MA, Halliday GM, Morris JGL. The Sydney multicenter study of Parkinson's disease: the inevitability of dementia at 20 years: twenty Year Sydney Parkinson's Study. *Mov Disord*. 2008;23(6):837-844. doi:10.1002/mds.21956
40. Melzer TR, Stark MR, Keenan RJ, et al. Beta amyloid deposition is not associated with cognitive impairment in Parkinson's disease. *Front Neurol*. 2019;10:391. doi:10.3389/fneur.2019.00391
41. Eckert T, Barnes A, Dhawan V, et al. FDG PET in the differential diagnosis of parkinsonian disorders. *NeuroImage*. 2005;26(3):912-921. doi:10.1016/j.neuroimage.2005.03.012
42. Meyer PT, Frings L, Rücker G, Hellwig S. ^{18} F-FDG PET in Parkinsonism: differential diagnosis and evaluation of cognitive impairment. *J Nucl Med*. 2017;58(12):1888-1898. doi:10.2967/jnumed.116.186403
43. Pappata S, Santangelo G, Aarsland D, et al. Mild cognitive impairment in drug-naive patients with PD is associated with cerebral hypometabolism. *Neurology*. 2011;77(14):1357-1362. doi:10.1212/WNL.0b013e3182315259
44. Heron CJL, Wright SL, Melzer TR, et al. Comparing cerebral perfusion in Alzheimer's disease and Parkinson's disease dementia: an ASL-MRI study. *J Cereb Blood Flow Metab*. 2014;34(6):964-970. doi:10.1038/jcbfm.2014.40
45. Hughes AJ, Daniel SE, Kilford L, Lees AJ. Accuracy of clinical diagnosis of idiopathic Parkinson's disease: a clinico-pathological study of 100 cases. *JNNP*. 1992;55(3):181-184. doi:10.1136/jnnp.55.3.181
46. MacAskill MR, Pitcher TL, Melzer TR, et al. The New Zealand Parkinson's progression programme. *J Roy Soc New Zealand*. 2023;53(4):466-488. doi:10.1080/03036758.2022.2111448
47. Wood KL, Myall DJ, Livingston L, et al. Different PD-MCI criteria and risk of dementia in Parkinson's disease: 4-year longitudinal study. *NPJ Parkinsons Dis*. 2016;2(1):15027. doi:10.1038/npjparkd.2015.27
48. Emre M, Aarsland D, Brown R, et al. Clinical diagnostic criteria for dementia associated with Parkinson's disease. *Mov Disord*. 2007;22(12):1689-1707. doi:10.1002/mds.21507
49. Litvan I, Goldman JG, Tröster AI, et al. Diagnostic criteria for mild cognitive impairment in Parkinson's disease: *movement* disorder society task force guidelines: PD-MCI Diagnostic Criteria. *Mov Disord*. 2012;27(3):349-356. doi:10.1002/mds.24893
50. Ashburner J, Friston KJ. Unified segmentation. *NeuroImage*. 2005;26(3):839-851. doi:10.1016/j.neuroimage.2005.02.018
51. Klunk WE, Koeppe RA, Price JC, et al. The Centiloid Project: standardizing quantitative amyloid plaque estimation by PET. *Alzheimer Dementia*. 2015;11(1):1. doi:10.1016/j.jalz.2014.07.003
52. Seibyl J, Catafau AM, Barthel H, et al. Impact of training method on the robustness of the visual assessment of ^{18} F-Florbetaben PET scans: results from a phase-3 study. *J Nucl Med*. 2016;57(6):900-906. doi:10.2967/jnumed.115.161927

53. Winkler AM, Ridgway GR, Webster MA, Smith SM, Nichols TE. Permutation inference for the general linear model. *NeuroImage*. 2014;92:381-397. doi:10.1016/j.neuroimage.2014.01.060
54. Smith S, Nichols T. Threshold-free cluster enhancement: addressing problems of smoothing, threshold dependence and localisation in cluster inference. *NeuroImage*. 2009;44(1):83-98. doi:10.1016/j.neuroimage.2008.03.061
55. Albrecht F, Ballarini T, Neumann J, Schroeter ML. FDG-PET hypometabolism is more sensitive than MRI atrophy in Parkinson's disease: a whole-brain multimodal imaging meta-analysis. *NeuroImage: Clinical*. 2019;21:101594. doi:10.1016/j.nicl.2018.11.004
56. Edison P, Ahmed I, Fan Z, et al. Microglia, amyloid, and glucose metabolism in Parkinson's disease with and without dementia. *Neuropsychopharmacol*. 2013;38(6):938-949. doi:10.1038/npp.2012.255
57. Garcia-Garcia D, Clavero P, Gasca Salas C, et al. Posterior parietooccipital hypometabolism may differentiate mild cognitive impairment from dementia in Parkinson's disease. *Eur J Nucl Med Mol Imaging*. 2012;39(11):1767-1777. doi:10.1007/s00259-012-2198-5
58. Berding G, Odin P, Brooks DJ, et al. Resting regional cerebral glucose metabolism in advanced Parkinson's disease studied in theoff andon conditions with [18F]FDG-PET. *Mov Disord*. 2001;16(6):1014-1022. doi:10.1002/mds.1212
59. Ottoy J, Verhaeghe J, Niemantsverdriet E, et al. ^{18}F-FDG PET, the early phases and the delivery rate of ^{18}F-AV45 PET as proxies of cerebral blood flow in Alzheimer's disease: validation against ^{15}O-H_2O PET. *Alzheimer Dementia*. 2019;15(9):1172-1182. doi:10.1016/j.jalz.2019.05.010
60. Al-Bachari S, Vidyasagar R, Emsley HC, Parkes LM. Structural and physiological neurovascular changes in idiopathic Parkinson's disease and its clinical phenotypes. *J Cereb Blood Flow Metab*. 2017;37(10):3409-3421. doi:10.1177/0271678X16688919
61. Pelizzari L, Di Tella S, Rossetto F, et al. Parietal perfusion alterations in Parkinson's disease patients without dementia. *Front Neurol*. 2020;11:562. doi:10.3389/fneur.2020.00562
62. Fernández-Seara MA, Mengual E, Vidorreta M, et al. Cortical hypoperfusion in Parkinson's disease assessed using arterial spin labeled perfusion MRI. *NeuroImage*. 2012;59(3):2743-2750. doi:10.1016/j.neuroimage.2011.10.033
63. Erro R, Ponticorvo S, Manara R, et al. Subcortical atrophy and perfusion patterns in Parkinson disease and multiple system atrophy. *Parkinsonism Relat Disord*. 2020;72:49-55. doi:10.1016/j.parkreldis.2020.02.009
64. Arslan DB, Gurvit H, Genc O, et al. The cerebral blood flow deficits in Parkinson's disease with mild cognitive impairment using arterial spin labeling MRI. *J Neural Transm*. 2020;127(9):1285-1294. doi:10.1007/s00702-020-02227-6
65. Lee TH, Huang KL, Chang TY, et al. Early-phase 18F-AV-45 PET imaging can detect crossed cerebellar diaschisis following carotid artery stenosis and cerebral hypoperfusion. *Curr Neurovasc Res*. 2017;14(3):258-265.
66. Melzer TR, Keenan RJ, Leeper GJ, et al. Test-retest reliability and sample size estimates after MRI scanner relocation. *NeuroImage*. 2020;211:116608. doi:10.1016/j.neuroimage.2020.116608
67. Chen Y, Wolk DA, Reddin JS, et al. Voxel-level comparison of arterial spin-labeled perfusion MRI and FDG-PET in Alzheimer disease. *Neurology*. 2011;77(22):1977-1985. doi:10.1212/WNL.0b013e31823a0ef7
68. Eidelberg D. Metabolic brain networks in neurodegenerative disorders: a functional imaging approach. *Trends Neurosci*. 2009;32(10):548-557. doi:10.1016/j.tins.2009.06.003
69. Ossenkoppele R, Prins ND, Pijnenburg YAL, et al. Impact of molecular imaging on the diagnostic process in a memory clinic. *Alzheimer Dementia*. 2013;9(4):414-421. doi:10.1016/j.jalz.2012.07.003
70. Asghar M, Hinz R, Herholz K, Carter SF. Dual-phase [18F]florbetapir in frontotemporal dementia. *Eur J Nucl Med Mol Imaging*. 2019;46(2):304-311. doi:10.1007/s00259-018-4238-2
71. Yong SW, Yoon JK, An YS, Lee PH. A comparison of cerebral glucose metabolism in Parkinson's disease, Parkinson's disease dementia and dementia with Lewy bodies: comparison of cerebral glucose metabolism in PD, PDD and DLB. *Eur J Neurol*. 2007;14(12):1357-1362. doi:10.1111/j.1468-1331.2007.01977.x
72. Juh R, Kim J, Moon D, Choe B, Suh T. Different metabolic patterns analysis of Parkinsonism on the 18F-FDG PET. *Eur J Radiol*. 2004;51(3):223-233. doi:10.1016/S0720-048X(03)00214-6
73. Loreto F, Fitzgerald A, Golemme M, et al. Prevalence of depressive symptoms in a memory clinic cohort: a retrospective study. *J Alzheimers Dis*. 2022;88(3):1179-1187. doi:10.3233/JAD-220170
74. Bohnen NI, Koeppe RA, Minoshima S, et al. Cerebral glucose metabolic features of parkinson disease and incident Dementia: longitudinal study. *J Nucl Med*. 2011;52(6):848-855. doi:10.2967/jnumed.111.089946
75. Beyer L, Nitschmann A, Barthel H, et al. Early-phase [18F]PI-2620 tau-PET imaging as a surrogate marker of neuronal injury. *Eur J Nucl Med Mol Imaging*. 2020;47(12):2911-2922. doi:10.1007/s00259-020-04788-w
76. Jin S, Oh M, Oh SJ, et al. Differential diagnosis of parkinsonism using dual-phase F-18 FP-CIT PET imaging. *Nucl Med Mol Imaging*. 2013;47(1):44-51. doi:10.1007/s13139-012-0182-4
77. Jin S, Oh M, Oh SJ, et al. Additional value of early-phase 18F-FP-CIT PET image for differential diagnosis of atypical parkinsonism. *Clinical Nuclear Medicine*. 2017;42(2):e80-e87. doi:10.1097/RLU.0000000000001474
78. Teune LK, Renken RJ, De Jong BM, et al. Parkinson's disease-related perfusion and glucose metabolic brain patterns identified with PCASL-MRI and FDG-PET imaging. *NeuroImage: Clinical*. 2014;5:240-244. doi:10.1016/j.nicl.2014.06.007
79. Goldman JG, Litvan I. Mild cognitive impairment in Parkinson's disease. *Minerva Med*. 2011;102(6):441-459.
80. Cheng L, Wu X, Guo R, et al. Discriminative pattern of reduced cerebral blood flow in Parkinson's disease and Parkinsonism-Plus syndrome: an ASL-MRI study. *BMC Med Imaging*. 2020;20(1):78. doi:10.1186/s12880-020-00479-y
81. Huang C, Mattis P, Perrine K, Brown N, Dhawan V, Eidelberg D. Metabolic abnormalities associated with mild cognitive impairment in Parkinson disease. *Neurology*. 2008;70(16):1470-1477. doi:10.1212/01.wnl.0000304050.05332.9c
82. Murakami N, Sako W, Haji S, et al. Differences in cerebellar perfusion between Parkinson's disease and multiple system atrophy. *J Neurol Sci*. 2020;409:116627. doi:10.1016/j.jns.2019.116627
83. Borghammer P, Cumming P, Aanerud J, Gjedde A. Artefactual subcortical hyperperfusion in PET studies normalized to global mean: lessons from Parkinson's disease. *NeuroImage*. 2009;45(2):249-257. doi:10.1016/j.neuroimage.2008.07.042

SUPPORTING INFORMATION

Additional supporting information can be found online in the Supporting Information section at the end of this article.

How to cite this article: Aye WWT, Stark MR, Horne K-L, et al. Early-phase amyloid PET reproduces metabolic signatures of cognitive decline in Parkinson's disease. *Alzheimer's Dement*. 2024;16:e12601. https://doi.org/10.1002/dad2.12601